



NEW ZEALAND SOCIETY FOR EARTHQUAKE ENGINEERING
**2019 Pacific Conference on
Earthquake Engineering**
TURNING HAZARD AWARENESS INTO RISK MITIGATION
4 – 6 April | SkyCity, Auckland | New Zealand



Experimental assessment of high-strength RC columns under different bi-directional loading protocols

S. Raza, S.J. Menegon, H.H. Tsang & J.L. Wilson

Department of Civil and Construction Engineering, Swinburne University of Technology, Melbourne Australia

ABSTRACT

In regions of lower seismicity, the design of buildings for earthquake actions is usually governed by very rare events of very low probability exceedance, which can still result in excessive seismic demands on structural components (e.g. columns, walls etc.) despite the low seismic nature of the region. One such demand is the bi-directional lateral motion of the building column, which significantly reduces the displacement capacity of the column, thereby making it more prone to collapse. This phenomenon of vulnerability to collapse seems to be of more concern in low to moderate seismic regions due to the adoption of limited ductile reinforced concrete construction in contrast to ductile construction prevalent in seismically active regions. Therefore, the primary aim of this study is to evaluate the seismic capacity or collapse performance of limited-ductile high-strength RC (HSRC) columns prevalent in regions of low to moderate seismicity under bi-directional displacement paths. To this end, this paper presents a comparative assessment of the seismic performance of two identical HSRC columns supporting an axial load ratio of $n=0.15$ and subjected to two different bi-directional loading paths.

1 INTRODUCTION

During an earthquake, the two orthogonal horizontal components of the ground motion result in bi-directional lateral displacement of the column. However, a large proportion of the experimental testing performed in literature investigates the seismic performance of reinforced concrete (RC) columns under uni-directional lateral loading conditions. A review of the existing literature revealed that only 58 RC columns have been tested under bi-directional loading paths in comparison to 378 RC columns tested under uni-directional loading conditions (Rodrigues et al. 2013b). Furthermore, the majority of the bi-directional experimental tests have been conducted on normal-strength RC columns with only one study being carried out on high-strength RC columns (Kuramoto et al. 1995). On the other hand, high-strength RC columns are

being widely used in high-rise constructions all over the world, which entails a better understanding of the seismic collapse performance of such columns under different bi-directional loading scenarios, due to the response dependency of the column on the type of the loading path.

Collapse performance of high-strength RC columns prevalent in regions of low to moderate seismicity (Australia, Canada etc.) should be of more concern in this regard as such columns possess low drift capacity (Raza et al. 2018a) due to the adoption of limited ductile detailing practice with considerably less confinement reinforcement as compared to the columns in regions of high seismicity. It should be noted that limited ductile detailing in the Australian context translates (loosely) to non-ductile detailing requirements of RC building codes in higher seismic regions (e.g. ACI 318-2014). Moreover, bidirectional loading also accelerates the strength and stiffness degradation (Bousias et al. 1995, Rodrigues et al. 2013a) and reduces the collapse drift capacity (drift corresponding to loss of axial load carrying capacity) of the column (Pham and Li 2013). Hence, a comprehensive experimental study is being conducted to assess the seismic collapse behaviour of limited ductile high-strength RC columns under bi-directional loading conditions. This paper presents a comparative assessment of the seismic performance of two identical columns tested under different bi-directional displacement paths as part of a larger experimental testing program of limited ductile HSRC columns the authors are currently performing.

2 DETAILS OF THE EXPERIMENTAL PROGRAM

The test matrix comprised of 14 HSRC column specimens, with axial load ratio, concrete compressive strength, confinement reinforcement and the loading paths being the variables of the study. The first six specimens are tested under uni-directional cyclic loading conditions with a constant axial load. The next six are tested under bi-directional loading conditions with a constant axial load and the last two are tested under bi-directional loading coupled with the variation of axial load. Table 1 summarizes the details of the test matrix. The specimens are provided with a limited ductile detailing representative of Australian construction practice (i.e. AS 3600). More details about the specimen design can be found in Raza et al. (2018b). Testing is conducted under state-of-the-art Multi-Axis Substructure Testing (MAST) facility at Swinburne University of Technology, Australia. Figure 1(a) shows the reinforcement and cross-sectional details of the column specimen and Figure 1(b) shows the specimen under the MAST system.

3 PROPOSED LOADING PROTOCOL

The choice of a realistic bi-directional loading protocol under pseudo static testing is of prime importance due to the response dependency of the RC columns on the imposed loading path. Previously, researchers have employed a number of bi-directional loading paths (Rodrigues et al. 2013b) but there is no guidance as to which protocol is representative of the actual displacement path of the column during an earthquake. The displacement path of the column is dependent on the coupling between the two orthogonal horizontal components of the ground motion. The unique and random characteristics of the different ground motions make it difficult to identify a smooth and regular displacement path of a column during earthquakes, but it is possible to generalize the displacement path of the column based on the observations of its displacement under a suite of ground motions with different characteristics. Thus, in order to select a bi-directional loading protocol representative of the actual displacement path of an RC column during an earthquake, a numerical study is conducted, the details of which are presented herein.

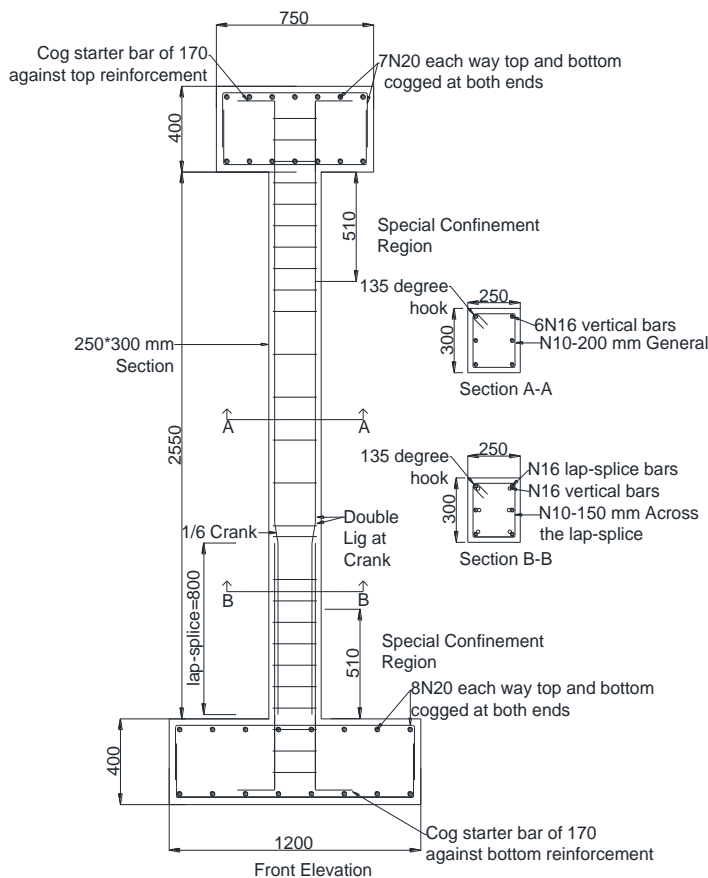
3.1 Numerical study

A cantilever HSRC column with the same material, reinforcement and cross-sectional properties as specimen S1 in Table 1 is subjected to a suite of scaled and unscaled 25 ground motions in OpenSees software (50 acceleration time history files) and the resulting displacement path is plotted. The amplitude of the ground

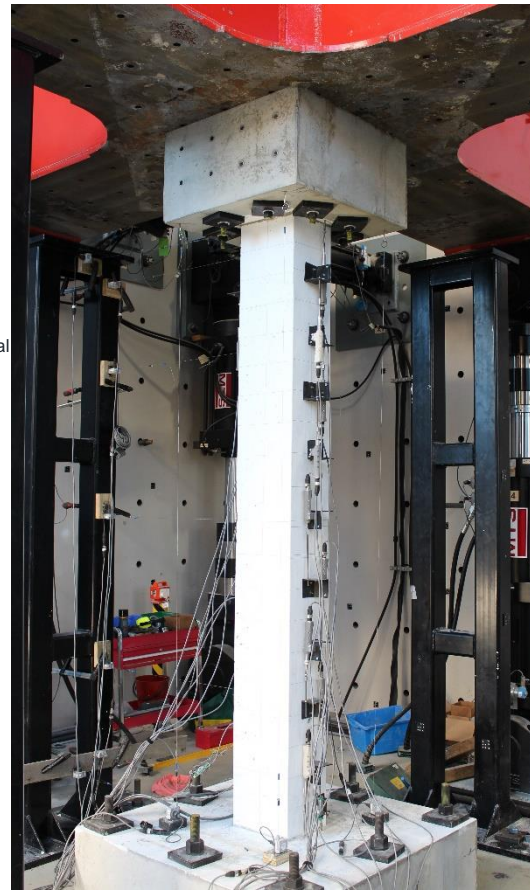
motions is scaled as such to produce some non-linear behaviour in the column. The specimen is subjected to ground motion accelerations in the X and Y directions only, and the displacement behaviour of the column is studied at an axial load ratio of 0.15. The ground motion accelerations considered in this study are obtained from PEER ground motion database (PEER 2013) and are representative of low to moderate seismic regions.

Table 1: Test Matrix

Specimen	Width × Depth × Height (mm)	Concrete Grade Strength f'_c (MPa)	Longitudinal Reinforcement ρ_v (%)	Stirrups (mm) ρ_h (%)	Axial Load Ratio n	Type of Loading
S1	250×300×2550	65.0	6N16(1.6%)	N10@150 (0.35%)	0.15	Uni-Directional
S2	250×300×2550	65.0	6N16(1.6%)	N10@150 (0.35%)	0.30	Uni-Directional
S3	250×300×2550	65.0	6N16(1.6%)	N10@150 (0.35%)	0.45	Uni-Directional
S4	250×300×2550	65.0	6N16(1.6%)	N10@100 (0.52%)	0.45	Uni-Directional
S5	250×300×2550	65.0	6N16(1.6%)	N10@300 (0.18%)	0.30	Uni-Directional
S6	250×300×2450	100.0	6N16(1.6%)	N10@150 (0.35%)	0.25	Uni-Directional
S7	250×300×2550	65.0	6N16(1.6%)	N10@150 (0.35%)	0.15	Bi-Directional (Linearized Circular)
S8	250×300×2550	65.0	6N16(1.6%)	N10@150 (0.35%)	0.30 ;	Bi-Directional (Linearized Circular)
S9	250×300×2550	65.0	6N16(1.6%)	N10@150 (0.35%)	0.15	Bi-Directional (Octo-Elliptical)
S10	250×300×2550	65.0	6N16(1.6%)	N10@150 (0.35%)	0.30	Bi-Directional (Octo-Elliptical- aspect ratio=0.3)
S11	250×300×2550	65.0	6N16(1.6%)	N10@150 (0.35%)	0.30	Bi-Directional (Octo-Elliptical- aspect ratio=0.5)
S12	250×300×2550	65.0	6N16(1.6%)	N10@150 (0.35%)	0.30	Bi-Directional (Hexagonal)
S13	250×300×2550	65.0	6N16(1.6%)	N10@150 (0.35%)	0.15±0.03	Bi-directional with variable axial load
S14	250×300×2550	100.0	6N16(1.6%)	N10@150 (0.35%)	0.25±0.05	Bi-Directional with variable axial load



(a)



(b)

Figure 1: a) Details of RC column (Dimensions in mm) b) Specimen under MAST

The ground motions are selected based on the following criteria: moment magnitude (M_w): 4.5-6.5, distance to rupture surface R_{rup} (km): 10-40 km and shear wave velocity: 180 m/s -1500 m/s. It is noted that the vertical component of the ground motion is not included in the analysis for the sake of simplicity. The displacement of the column in the X and Y directions is plotted against each other to view the bi-directional lateral displacement path of the column under each ground motion. The displacement path of the column under unscaled and scaled Christchurch (2011) ground motions is shown as an illustration in Figure 2. It can be seen that the biaxial displacement path of the column generally comprised of loops of different orientations and aspect ratios. More or less similar behaviour is observed for the other ground motions, with the diagonal orientation of the loops being predominantly observed in the displacement path of the column. The different orientations of the loops can be attributed to the phase shift between X and Y-axis displacement of the column.

3.2 Development of bi-directional loading protocol

Based on the results of the numerical study, two bi-directional loading protocols, namely linearized circular path and octo-elliptical path are proposed. Figure 3(a) shows the linearized circular displacement path. The linearized circular path was developed from a linearized elliptical loading protocol used in the experimental testing program of RC walls performed by researchers at the University of Auckland (Hogan et al. 2018). It consists of a linearized quarter of a circle in each quadrant. Each quarter circle starts and finishes at the origin. The column is first displaced in the first quadrant, from where it goes to the third quadrant and then to second and fourth quadrants, respectively, before finally finishing back at the origin. After completion of one cycle of the quarter circles, the specimen is subjected to a second cycle of quarter circles in all the quadrants for

capturing the strength and stiffness degradation under repeated displacement excursions, thereby resulting in a total of 8 quarter circles. This protocol is a relatively simple approximation of the displacement path of the column observed in the numerical study and primarily displaces the column in the diagonal quadrants.

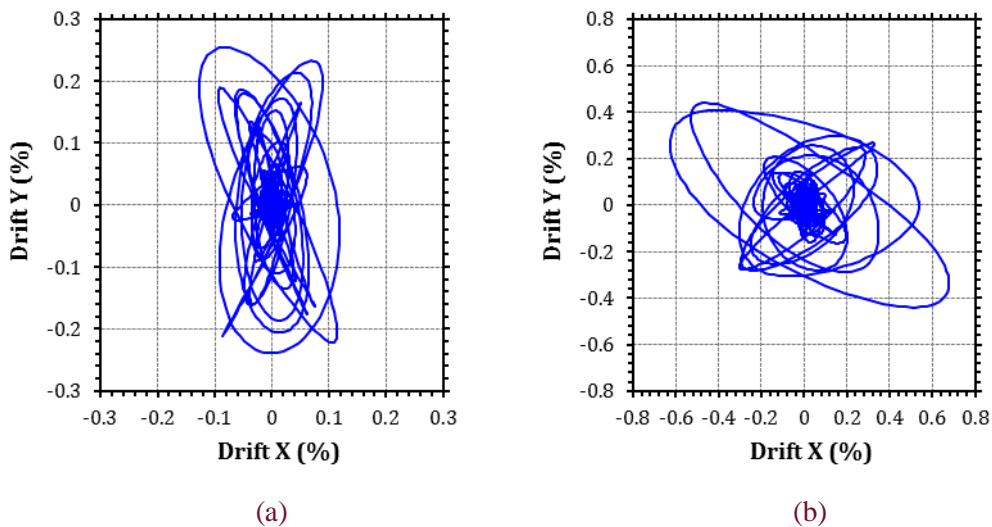


Figure 2: Lateral displacement path of the column under ground motion a) Christchurch (Unscaled) b) Christchurch (Scaled)

On the other hand, the octo-elliptical loading path shown in Figure 3(b), is a more sophisticated bi-directional protocol which attempts to generalize the actual displacement path of the column under ground motions using elliptical loops of different orientations. The octo-elliptical path is comprised of eight elliptical loops, with the first four displacing the column in the counter clockwise direction, and the last four displacing it in the clockwise direction. The aspect ratio (a/b) of the ellipses is $1/3$. The octo-elliptical path begins with a vertical ellipse that displaces the column in the Y-direction from the origin. The completion of the vertical ellipse is followed by the diagonal movement of the column in the counter clockwise direction using a diagonal ellipse, which is then followed by the displacement in the X-direction utilizing a horizontal ellipse. Finally, the fourth and the last ellipse of the counter clockwise cycle displaces the column diagonally again before bringing it back to the origin. After finishing one complete cycle of displacements in the counter clockwise direction, the four ellipses are repeated again but this time in the clockwise direction. In

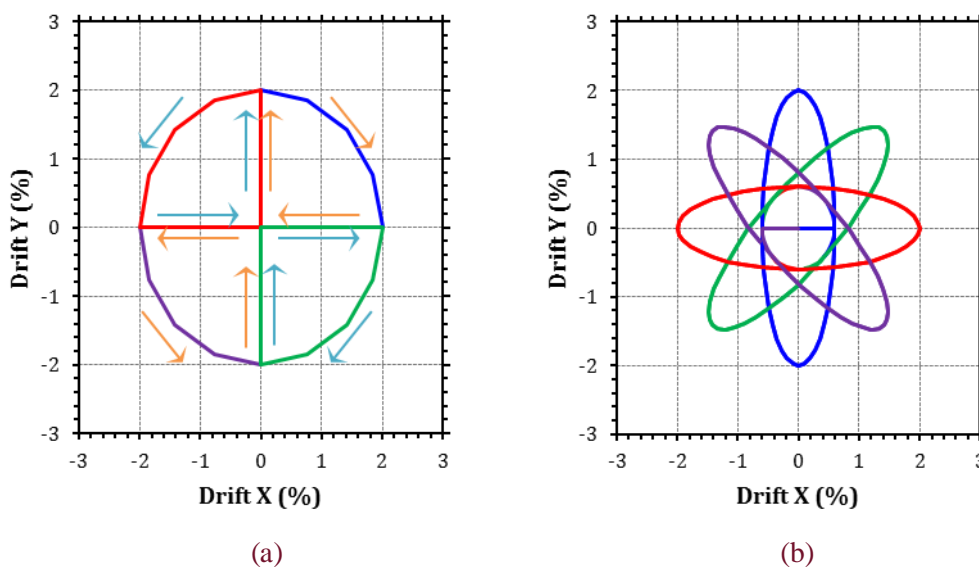


Figure 3: Proposed Bi-Directional Protocols a) Linearized Circular b) Octo-elliptical

this loading protocol, a smooth transition is provided for moving from one ellipse to another using arcs. The two small semi circles around the origin are due to the provision of these arcs. The upper semicircle is formed when the ellipses are moving in the counter clockwise direction, whereas lower semicircle is formed during the displacement in the clockwise direction.

4 EXPERIMENTAL RESULTS AND DISCUSSION

This section presents the results of two identical specimens, S7 and S9 from Table 1, supporting an axial load ratio of $n=0.15$ and tested under two different bi-directional displacement paths; the former being tested under linearized circular path and the latter under octo-elliptical path. The concrete cylinder strength for specimens S7 and S9 are 86 MPa and 90 MPa, respectively. A comparative assessment of the results is performed in terms of the force-displacement behaviour and hysteretic energy dissipation of the column specimens under the proposed testing protocols.

4.1 Force-Displacement Behaviour

The hysteretic curves of the specimens S7 and S9 in the X and Y directions are shown in Figures 4(a), 4(b) and 5(a), 5(b), respectively. By and large, the two displacement protocols resulted in almost identical force-displacement characteristics. The lateral strength of the two columns can be observed to be more or less similar in X and Y directions. The specimens also collapsed at the same drift value of 2.4%. Specimen S7 was able to sustain a displacement excursion of 2.4% in the first and the third quadrants of the linearized circular path and collapsed while entering the 2nd quadrant. On the other hand, specimen S9 sustained four counter clockwise ellipses and two clockwise ellipses during the cycle with the peak displacement excursion of 2.4%. This apparently means that octo-elliptical path is comparatively less severe than the linearized circular path. However, it is worth noting that the peak positive and negative displacement excursions in the X and Y directions are repeated four times in the linearized circular displacement path (ref Figure 3(a)), with the first two times during the first cycle of quarter circles in each quadrant and the remaining two times during the second cycle. In contrast, the peak positive and negative displacements in X and Y directions are repeated only twice in the octo-elliptical path, since the column experiences less displacement than the peak value in the diagonal ellipses of the protocol (ref Figure 3b).

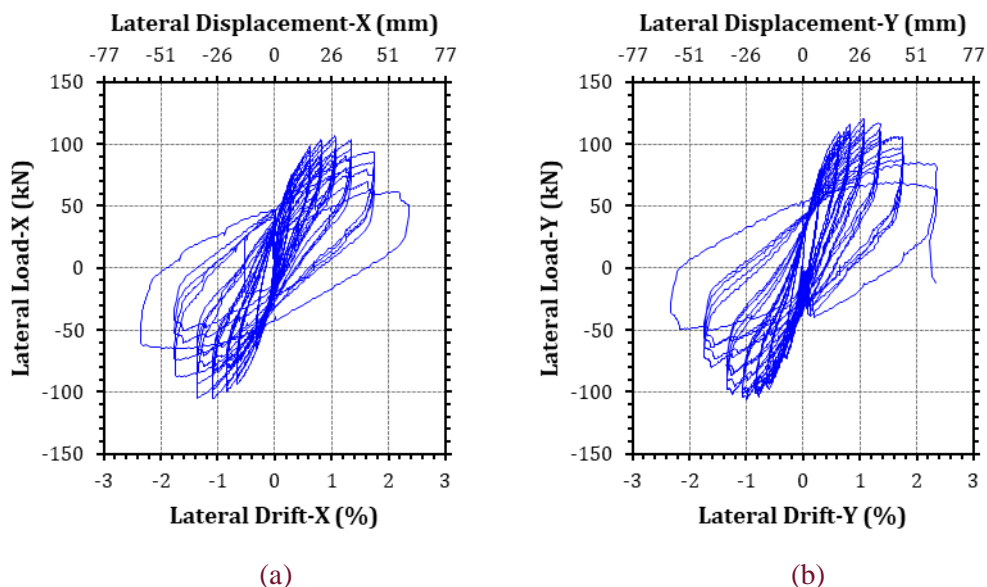


Figure 4: Hysteretic curves under linearized circular displacement path a) S7 (X-direction) b) S7 (Y-direction)

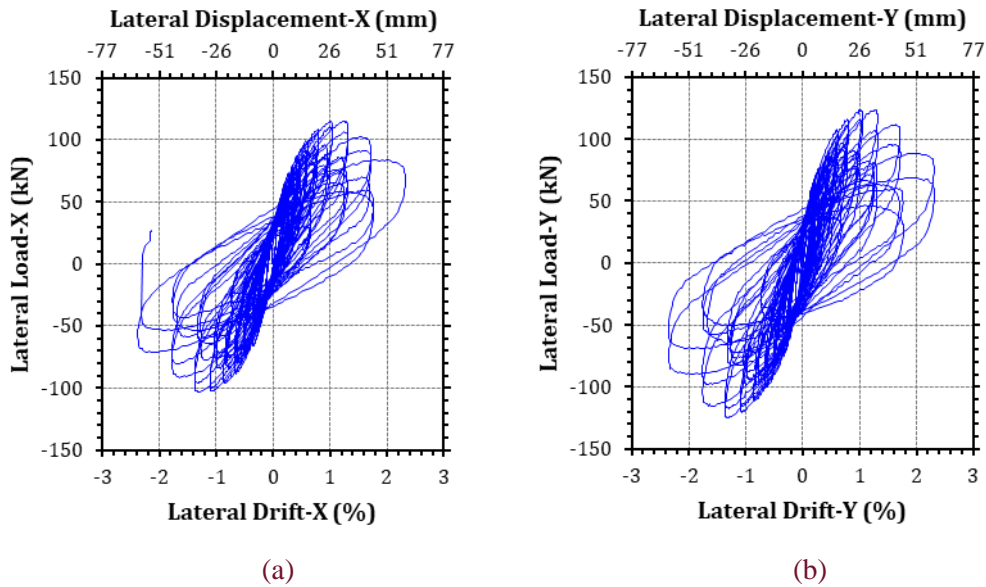


Figure 5: Hysteretic curves under octo-elliptical displacement path a) S9 (X-direction) b) S9 (Y-direction)

4.2 Hysteretic Energy Dissipation

The seismic behaviour of the specimens is also compared by evaluating the hysteretic energy dissipation of the specimens. The area enclosed by the force-displacement hysteresis is computed to determine the hysteretic energy dissipation of the specimens. The energy dissipation for each individual cycle in X and Y directions is given by:

$$E_{dx} = \int F(x)dx \quad \& \quad E_{dy} = \int F(y)dy$$

where, E_{dx} , E_{dy} , $\int F(x)dx$ and $\int F(y)dy$ denote energy dissipation and area under the force-displacement hysteresis, respectively, in the X and Y directions. Figures 6 (a) and (b) show the variation of energy dissipation of the specimens S7 and S9 with the increasing lateral drifts in the X and Y directions. It can be observed that energy dissipation of the two specimens is nearly the same at small displacement excursions, however, at large displacement excursions the energy dissipation of the specimen tested under linearized circular path is slightly greater than that of the specimen tested under octo-elliptical path, which would imply that octo-elliptical path reduces the energy dissipation capacity of the column.

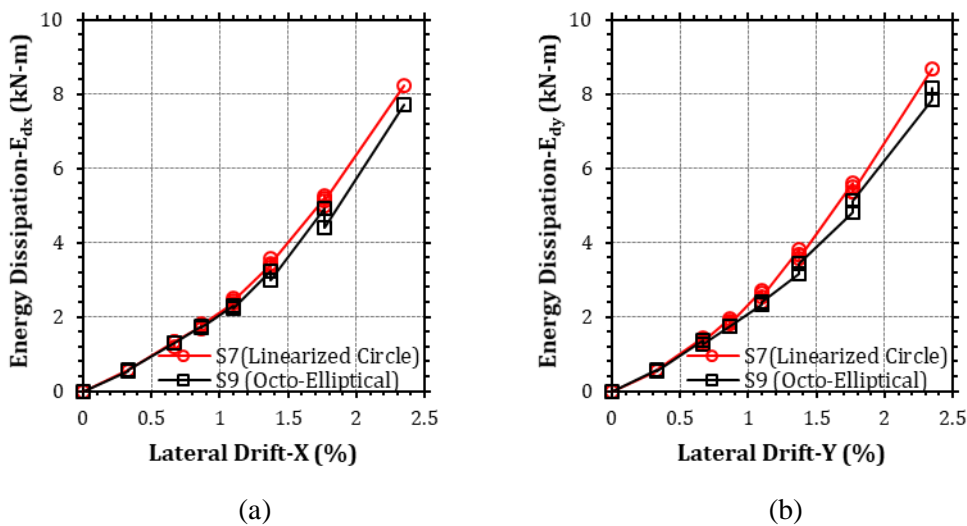


Figure 6: Hysteretic Energy Dissipation a) S7 & S9 (X-direction) b) S7 & S9 (Y-direction)

5 CONCLUSIONS

This paper presents a comparative assessment of the seismic collapse performance of two identical columns tested under two different bi-directional loading protocols, namely linearized circular path and octo-elliptical path. The linearized circular path is an extension of a loading protocol used by researchers in an experimental testing of RC walls at the University of Auckland and the octo-elliptical path is developed by the authors based on the results of a numerical study conducted to investigate the bi-directional lateral displacement path of the column under ground motions of different characteristics. The paper compared the proposed bi-directional loading protocols in terms of the force-drift behaviour and energy dissipation capacity of the tested columns. It was observed that the collapse drift capacity (axial load failure drift) of both the columns was same under the two displacement paths, however, the specimen tested under linearized circular path exhibited 6-10% more energy dissipation for drifts > 1.0% compared to the specimen tested under octo-elliptical path. This implies that octo-elliptical path, which is also a more realistic representation of the actual displacement path of the column during an earthquake, reduces the energy dissipation capacity of the column. Further experimental study and analysis is recommended to arrive at some definite conclusions in this regard.

6 ACKNOWLEDGEMENTS

The authors greatly acknowledge Bushfire and Natural Hazards CRC for providing financial support and Swinburne Smart Structures Lab staff for providing technical assistance during the experimental tests.

7 REFERENCES

- ACI Committee 318, 2014. *Building Code Requirements for Structural Concrete (ACI 318M-14) and commentary (ACI 318RM-14)*, American Concrete Institute, Farmington Hills, MI.
- Bousias, S. N., Verzeletti, G., Fardis, M. N., Gutierrez, E. 1995. Load-Path Effects in Column Biaxial Bending with Axial Force, *Journal of Engineering Mechanics*, vol. 121 (5) 596-605.
- Hogan, L. S., Henry, R. S., & Ingham, J. M. 2018. Performance of panel-to-foundation connections in low-rise precast concrete buildings. *Journal of the Structural Engineering Society of New Zealand*, vol. 31 (1) 26-36.
- Kuramoto, H., Kabeyasawa, T., Shen, F.-H. 1995. Influence of Axial Deformation on Ductility of High-Strength Reinforced Concrete Columns Under Varying Triaxial Forces, *Structural Journal*, vol. 92 (5)
- PEER 2013. Pacific Earthquake Engineering Research (PEER) Center Ground Motion Database.
- Pham, T. P., Li, B. 2013. Seismic Behavior of Reinforced Concrete Columns with Light Transverse Reinforcement under Different Lateral Loading Directions, *Structural Journal*, vol. 110 (5).
- Raza, S., Tsang, H.-H., Wilson, J. L. 2018a. Unified models for post-peak failure drifts of normal- and high-strength RC columns, *Magazine of Concrete Research*, vol. 70 (21) 1081-1101.
- Raza, S., Menegon, S., Tsang, H.-H., Wilson, J. L. 2018b. Experimental Testing Program to Investigate the Collapse Drift Capacity of Limited Ductile High-Strength RC Column, *Proceedings of the 25th Australasian Conference on the Mechanics of Structures and Materials, ACMSM25*, Brisbane, Australia.
- Rodrigues, H., Arêde, A., Varum, H., Costa, A. G. 2013a Experimental Evaluation of Rectangular Reinforced Concrete Column Behaviour under Biaxial Cyclic Loading, *Earthquake Engineering & Structural Dynamics*, vol. 42 (2) 239-259.
- Rodrigues, H., Varum, H., Arêde, A., Costa, A. G. 2013b. Behaviour of Reinforced Concrete Column under Biaxial Cyclic Loading—State of the Art, *International Journal of Advanced Structural Engineering*, vol. 5 (4).
- Standards Australia, 2018. AS 3600-2018 *Concrete structures*, SAI Global Limited, Sydney.